

Somatotopic Organization of the Corticospinal Tract in the Human Brainstem: A MRI-Based Mapping Analysis

Juergen J. Marx, MD,¹ Gian D. Iannetti, PhD,² Frank Thömke, MD,¹ Sabine Fitzek, MD,³ Peter P. Urban, MD,¹ Peter Stoeter, MD,⁴ Giorgio Cruccu, MD,² Marianne Dieterich, MD,¹ and Hanns C. Hopf, MD¹

To investigate the incompletely understood somatotopic organization of the corticospinal tract in the human brainstem, we performed a voxel-based statistical analysis of standardized magnetic resonance scans of 41 prospectively recruited patients with pyramidal tract dysfunction caused by acute brainstem infarction. Motor hemiparesis was rated clinically and by the investigation of motor evoked potentials to arms and legs. Infarction affected the pons in 85% of cases. We found the greatest level of significance of affected brainstem areas between the pontomesencephalic junction and the mid pons. Lesion location was significantly more dorsal in patients with hemiparesis affecting more proximal muscles and was significantly more ventral in patients with predominantly distal limb paresis. Comparison of magnetic resonance lesion from patients with paresis predominantly affecting arm or leg did not show significant topographical differences. We conclude that a topographical arm/leg distribution of corticospinal fibers is abruptly broken down as the descending corticospinal tract traverses the pons. Corticospinal fibers, however, follow a somatotopic order in the pons with fibers controlling proximal muscles being located close to the reticular formation in the dorsal pontine base, and thus more dorsal than the fibers controlling further distal muscle groups.

Ann Neurol 2005;57:824–831

The anatomical pathway of the pyramidal tract and its somatotopic organization in the cortex and the internal capsule has been intensively studied and is widely accepted.^{1–4} In contrast, the location of the corticospinal tract and a possible somatotopic order of its fibers in the human brainstem is far less known.^{5–8} Anatomical-functional correlation studies are particularly difficult in the brainstem because of the close proximity of nuclei and fiber tracts. Lesion studies in experimental animals and a few human cases indicate a clear somatotopic order of the pyramidal tract in the internal capsule and at least in the upper brainstem, with fibers directed to the arm running more anteromedially and fibers directed to the leg more dorsolaterally.^{4,9–11} Fibers of the arm and leg appear to overlap progressively within the lower brainstem.^{9,10,12} According to earlier autoradiographic tracer and lesion studies in the rhesus monkey, fibers supplying more distal muscle groups, especially of the hands, are supposed to run further laterally in the lower brainstem than those controlling ax-

ial and proximal extremity movements.^{13–15} Although neuroradiological imaging advanced considerably in the last decade, the exact localization of the corticospinal projections through the human brainstem remains unclear. Currently, anatomical-functional correlation studies using postmortem specimens or neuroimaging are still anecdotal and based on a restricted number of samples providing qualitative, rather than quantitative, statistically supported results.

To investigate the anatomical pathway and the somatotopic organization of the corticospinal tract through the human brainstem, we analyzed the topography of magnetic resonance (MR) lesions in prospectively recruited patients with acute brainstem infarction and acute motor hemiparesis demonstrated by clinical and electrophysiological (motor-evoked potentials [MEPs]) abnormalities. MR scans were imported and normalized into a voxel-based model of the human brainstem, and statistical analysis of lesion location was performed. This new technique of three-dimensional

From the ¹Departments of Neurology, Johannes Gutenberg-University Mainz, Mainz, Germany; ²Department of Neurosciences, University of Rome, "La Sapienza," Rome, Italy; ³Department of Neurology, Friedrich Schiller-University Jena, Jena, Germany; and ⁴Department of Neuroradiology, Johannes Gutenberg-University Mainz, Mainz, Germany.

Received Nov 15, 2004, and in revised form Feb 28, 2005. Accepted for publication Mar 13, 2005.

Published online Apr 25, 2005, in Wiley InterScience (www.interscience.wiley.com). DOI: 10.1002/ana.20487

Address correspondence to Dr Marx, Department of Neurology, University of Mainz, Langenbeckstr. 1, D-55101 Mainz, Germany. E-mail: marx@neurologie.klinik.uni-mainz.de

brainstem mapping has been demonstrated to be useful in earlier structural-functional correlation studies in the human brainstem.^{16–18}

Patients and Methods

Between 1998 and 2001, we prospectively recruited 258 consecutive patients with acute signs and symptoms of vertebrobasilar ischemia. Inclusion criteria were acute ocular motor disorders, cranial nerve dysfunction, and limb or gait ataxia as indicators of acute vertebrobasilar dysfunction. Patients underwent magnetic resonance imaging (MRI) following a fixed protocol (see later).

In 41 of these patients (16%), MRI and complementary investigations such as electrooculography or lumbar puncture finally indicated a diagnosis other than brainstem infarction, for example, peripheral vestibulopathy (7 patients), pure cerebellar infarction (7 patients), intracerebral hemorrhage (5 patients), brainstem tumor, inflammatory disease, and others. Fifty-three (24%) of the remaining 217 patients with “best final diagnosis” brainstem infarction had motor hemiparesis. Other frequent symptoms were gait ataxia (61%), cranial nerve lesions (29%), dysarthria (24%), and oculomotor disorders (21%).

In 71.4% of these patients (155/217), MRI indicated acute brainstem infarction. Forty-four of these patients (28.4%) showed acute motor hemiparesis caused by MRI-documented brainstem infarction (see later for clinical criteria of central paresis). Three of these patients had multiple acute brainstem infarctions, which made structural-functional correlations impossible. Thus, 41 patients with acute motor paresis caused by isolated acute brainstem infarction documented by MRI remained for further correlation analysis.

MEPs were investigated within 7 days from the onset of clinical symptoms, and at least one follow-up investigation was done after 2 weeks.

Approval of the study was granted by the university ethics committee, and patients gave informed consent to the procedures.

Clinical Investigation

Detailed clinical investigation was done within 24 hours after onset of symptoms. The clinical diagnosis of hemiparesis implied either motor weakness or clear drift of held arm or leg towards the bed within 5 seconds in standard neurological investigation. Pure hyperreflexia or Babinski sign were not rated as sufficient clinical criteria.

Patients with motor hemiparesis were grouped according to the predominantly affected limb and the proximal-distal location of the hemiparesis as apparent from clinical investigation. If a predominantly affected limb could not be identified by clinical investigation alone, results of MEPs were used to assign the patients to the “arm” or “leg” group.

Motor-Evoked Potentials

MEP investigations were done in all but 3 of the 41 selected patients within 1 week after onset of symptoms. A circular coil (mean diameter, 9cm; peak magnetic field, 2.0 Tesla; Magstim 200S; Novametrix, Bristol, United Kingdom) was used for stimulation. Electromyographic recordings were

taken bilaterally from upper and lower limb muscles using standard procedures: surface electrodes were placed on the musculus abductor digiti minimi and the musculus tibialis anterior, respectively. To allow calculation of a central conduction time, we performed magnetic stimulation of the spinal roots with the coil placed over the lower cervical spine and the lower lumbar spine. For cortical stimulation, the center of the coil was positioned tangentially at the vertex (upper limbs) and 4 cm in front of the vertex (lower limbs). Stimulation strength was increased stepwise during slight preinnervation until stable latencies were achieved. We measured four successive responses per muscle and took the shortest onset latency and largest peak-to-peak amplitude as MEP measures. Absolute values for latencies, amplitudes, central conduction time, and side differences were evaluated according to our previously reported normal values.^{19,20} Reference limits are given in Table 1.

MEPs were applied to assign patients to the arm or leg group, if this decision could not be made clinically. Responses were classified on a three-level ranking of abnormality: normal, abnormal (delayed latency or reduced amplitude), or absent response.

Magnetic Resonance Imaging Acquisition and Postprocessing

Biplanar T2- and diffusion-weighted MRI was done within 48 hours after onset of symptoms with a 1.5 Tesla superconducting system (Magnetom Vision; Siemens, Erlangen, Germany). We used diffusion-weighted echo planar imaging (TR, 4,000 milliseconds; TE, 103 milliseconds) with separately applied diffusion gradients in the three spatial axes ($b = 1,164\text{sec}/\text{mm}^3$; 128×128 matrix; 250 milliseconds per slice; 20 slices; thickness, 3mm; 8 measurements). Axial and sagittal high-resolution T2- (TR, 3,810 milliseconds; TE, 90 milliseconds; 256×256 matrix; slice thickness, 3mm) and T1-weighted imaging (TR, 600 milliseconds; TE, 14 milliseconds; 256 matrix; slice thickness, 3mm) before and after intravenous gadolinium was done as soon as patients could tolerate the longer lasting MRI scan (median, 6.5 days after onset of symptoms). Slice orientation was parallel (sagittal sections) and perpendicular (axial sections) to the sagittal brainstem cuts of the stereotactic anatomical atlas of Schaltenbrand and Wahren²¹ (Fig 1).

Three-Dimensional Mapping and Statistics

The area of infarction was identified independently by two neuroradiologists and one neurologist. The same image was zoomed, scaled, rotated, and nonlinearly warped to be normalized to the proper level of the model according to the brainstem outlines and anatomical landmarks such as the fourth ventricle or the exit zones of cranial nerves. Each image was flipped top-bottom (to comply with the anatomical atlas representation) and right-left if the area of abnormal signal was right-sided (to have the lesions of all patients on one side), and finally imported in our model.

This is a voxel-based three-dimensional brainstem model^{15,18,22} developed using data from several topometric and stereotactic atlases^{21,23,24} (Fig 2). It is subdivided into 5,268 volume elements (“voxels”) ranging from $2 \times 2 \times 2\text{mm}$ to $2 \times 2 \times 4\text{mm}$. After MR images were imported,

Table 1. Limits of the Norm of MEPs from the Limb Muscles

Body Height (cm)	TMCT (msec)	PMCT (msec)	CMCT (msec)	Δ CMCT (msec)	MEP/M Wave Ratio (%)
Upper limbs (ADM)					
<170	23.4	15.5	10.1	2.4	15
171–180	24.7	16.2	9.8	2.1	
>180	24.9	17.0	10.0	3.5	
Lower limbs (TA)					
<170	32.1	15.8	18.7	3.4	10
171–180	32.5	16.8	19.0	2.4	
>180	35.9	18.0	18.9	3.4	

ADM = abductor digiti minimi muscle; TA = tibial anterior muscle; TMCT = total motor conduction time (cortex-muscle); PMCT = peripheral motor conduction time (root-muscle); CMCT = central motor conduction time (cortex-root); Δ CMCT = interside difference of CMCT; MEP/M wave ratio = amplitude ratio between motor cortex response and M-wave amplitude with electrical stimulation of the distal peripheral nerve.

each voxel of the brainstem was assigned a value of 0, 0.5, or 1 for every lesion; value 1 represented a voxel certainly affected by the lesions, value 0 represented a voxel certainly unaffected, and value 0.5 represented a voxel only partially affected by the lesion. Statistical analysis of the pooled patient data aimed to identify which of the 5,268 voxels were affected in a patient group (within-group, one-sample analysis), or which voxels differed significantly in two patient groups (two-sample analysis). For within-group analysis, the system performed χ^2 test. For each voxel, the statistical probabilities for a voxel affected in the patient group were calculated separately against a hypothetical mean value of the probability of a casual lesion in this voxel, provided by the average number of affected voxels in our population. For the two-sample statistical analysis between two patient groups, the Mann-Whitney *U* test was applied in every voxel separately. The significance of the statistical test result was color-coded according to the achieved *p* value in each voxel and displayed at its proper location in the brainstem model, creating a three-dimensional (3D) statistical map. The statistical significance was color-coded in each voxel from blue (non-significant), to white (affected with low significance, $p < 0.05$), to red (affected with greatest significance, $p < 0.0005$) with intermediate colors and displayed at its proper location in the brainstem model. This created a 3D parametric map of the statistical result. From the 3D visualization, 2D slices can be extracted along any of the three main section planes and can be further elaborated to smooth the boundaries.

Results

Forty-one of the prospectively recruited patients showed an acute clinical lesion of the pyramidal tract contralateral to acute isolated brainstem infarction documented by MRI. All but 2 of the 38 patients to whom MEP investigations were applied showed corresponding electrophysiological abnormalities of a corticospinal tract lesion. Fifteen were male patients and 26 were female patients. Age ranged from 26 to 87 years (mean age, 67.1 years). About 4.9% of these patients had mesencephalic infarction, 17.1% had pontomesencephalic, 58.5% had pontine, 9.8% had pontomedul-

lary, and 9.8% had medullary ischemia. Clinical data are given in Table 2.

Sonography and MR angiography detected occlusion or stenosis of the vertebral artery in six patients.

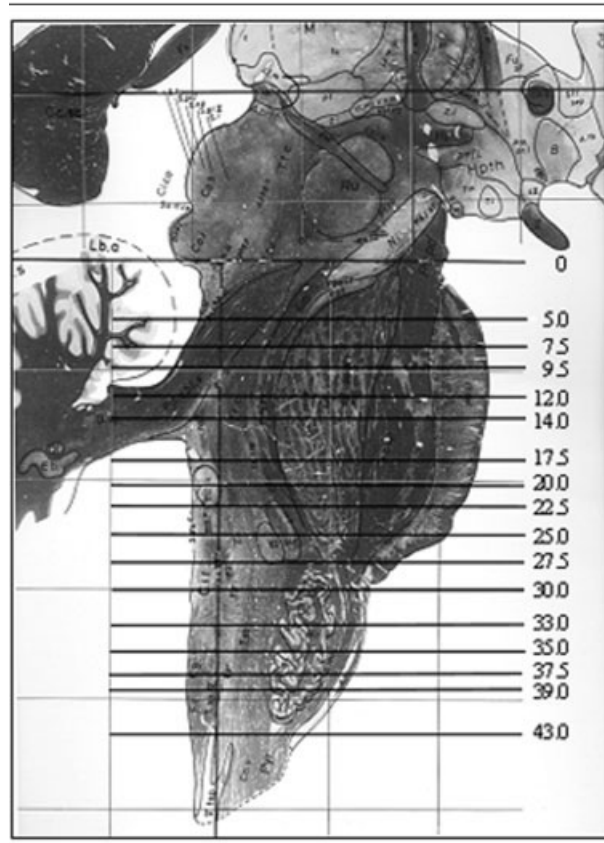


Fig 1. Sagittal view of the brainstem according to the anatomical atlas of Schaltenbrand and Wahren.²¹ Orientation of magnetic resonance imaging scans was done parallel and perpendicular to the axial slices shown. Numbers represent the distance from the pontomesencephalic junction (zero point) in millimeters in craniocaudal direction.

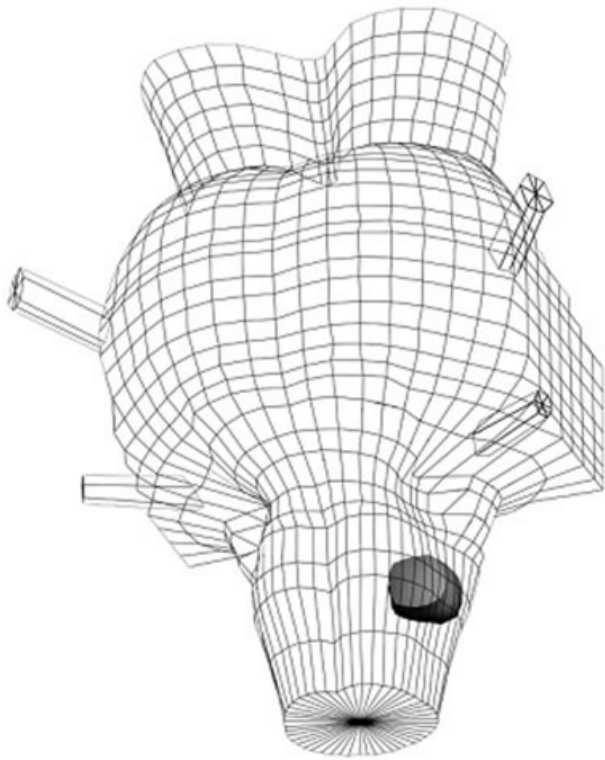


Fig 2. Example of an ischemic lesion in the dorsolateral medulla oblongata after normalization and import into the three-dimensional brainstem model.

Twenty-eight patients had multiple vascular risk factors, and sonography demonstrated macroangiopathy of the internal carotid artery but no vertebral stenosis or occlusion. In seven patients, the cause of the infarction remained unclear.

The statistical analysis of lesion location in these patients with motor hemiparesis as compared with the 111 patients in our study without paresis proved an area in the upper ventral to medial pons to be significantly associated with motor hemiparesis. This corresponds to earlier imaging studies on brainstem lesions causing corticospinal tract dysfunction.^{4,8,11} The corticospinal tract as depicted in the stereotactic atlas of Schaltenbrand and Wahren²¹ was affected by the lesion of every patient with motor hemiparesis (Fig 3).

The hemiparesis was more pronounced in the arm in 20 patients and in the leg in 7. In 14 patients, there was no clinical or MEP difference between arm and leg. In 17 patients, the hemiparesis was more pronounced in distal muscles of the arm and leg; in 14 patients, the hemiparesis was more pronounced in proximal muscles. Ten patients showed no proximal or distal predominance of paresis (Table 3).

Statistical evaluation of the lesion location in the patients with predominantly distal and proximal muscle paresis showed for both patient groups significantly af-

Table 2. Most Frequent Clinical Signs Associated with Hemiparesis Due to Brainstem Infarction (n = 41)

Clinical Sign	No. (%)
Dysarthria	20 (58.8)
Gait ataxia	18 (43.9)
Facial paresis	14 (34.1)
Cranial nerve lesions	11 (26.8)
N. III	3 (7.3)
N. V	5 (12.2)
Ocular motor disorder	8 (19.5)
Skew deviation	3 (7.3)
Pathological nystagmus	3 (7.3)
Internuclear ophthalmoplegia	6 (14.6)

ected areas on transversal atlas sections from the pontomesencephalic junction to mid pons ($p < 0.05$). Significant voxels were located near the midline for both groups and overlapped the pyramidal tract marked in the atlas. In a two-sample analysis comparing the lesion location in both groups (Mann-Whitney U test), the affected area was significantly more dorsal and lateral in patients with hemiparesis involving more proximal muscle groups and was significantly more ventral in patients with predominantly distal muscle limb paresis ($p < 0.02$; Fig 4).

For patients with hemiparesis predominantly affect-

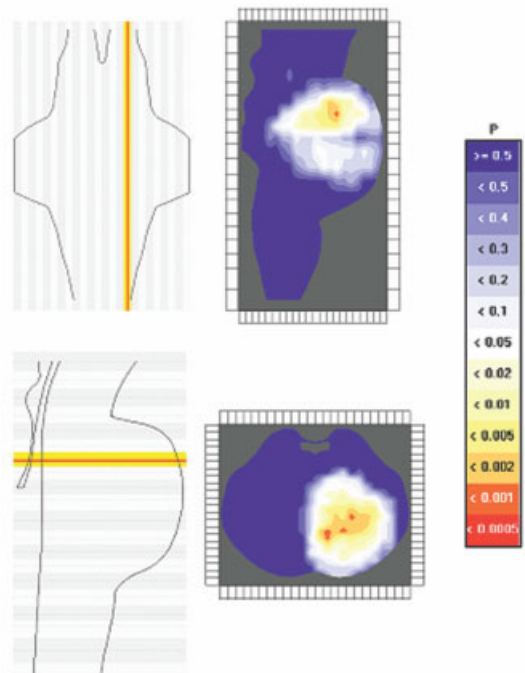


Fig 3. Color-coded probability maps on sagittal view and the axial pontine section with greatest significance of affected voxels in the three-dimensional brainstem model, comparing the 44 patients with and 111 patients without clinical motor hemiparesis caused by brainstem infarction (Mann-Whitney U test).

Table 3. Assignment to Subgroups of Hemiparesis for Statistical Comparison according to Findings in Clinical Examination and Motor-Evoked Potentials (n = 41)

Predominance	Clinically	No Clinical Predominance, but according to MEP	Clinically and/or MEP
Arm predominance	13	7	20 (48.8%)
Leg predominance	3	4	7 (17.1%)
No predominance	25	14	14 (34.1%)
Proximal predominance	17 (41.5%)	—	—
Distal predominance	14 (34.1%)	—	—
No predominance	10 (24.4%)	—	—

MEP = motor-evoked potential.

ing the arm, a significant area was found in the upper pons corresponding to the anatomical transversal atlas slices located 5 to 9.5 mm distal to the pontomesencephalic junction. This area was also located rather medial and dorsal ($p < 0.05$). Significantly affected voxels in patients with leg predominant hemiparesis appeared to lie above, within, and below this location (Fig 5). A two-sample analysis comparing affected voxels in patients with arm or leg predominance of paresis, however, did not indicate a significant difference in lesion location anywhere in the whole brainstem as depicted in the coronal view and on the transversal pontine atlas

slice with highest lesion density in Figure 5. Statistical calculations indicated a nonsignificant trend to a more medial lesion location in patients with arm predominance of paresis in the upper pons near the pontomesencephalic junction, which accordingly cannot be displayed in the color-coded parametric maps.

Discussion

Information on the course of the corticospinal tract through the human brainstem is rare and incomplete.^{4,7,8,11,25} In the few available studies, little has been reported on a possible somatotopical order of the

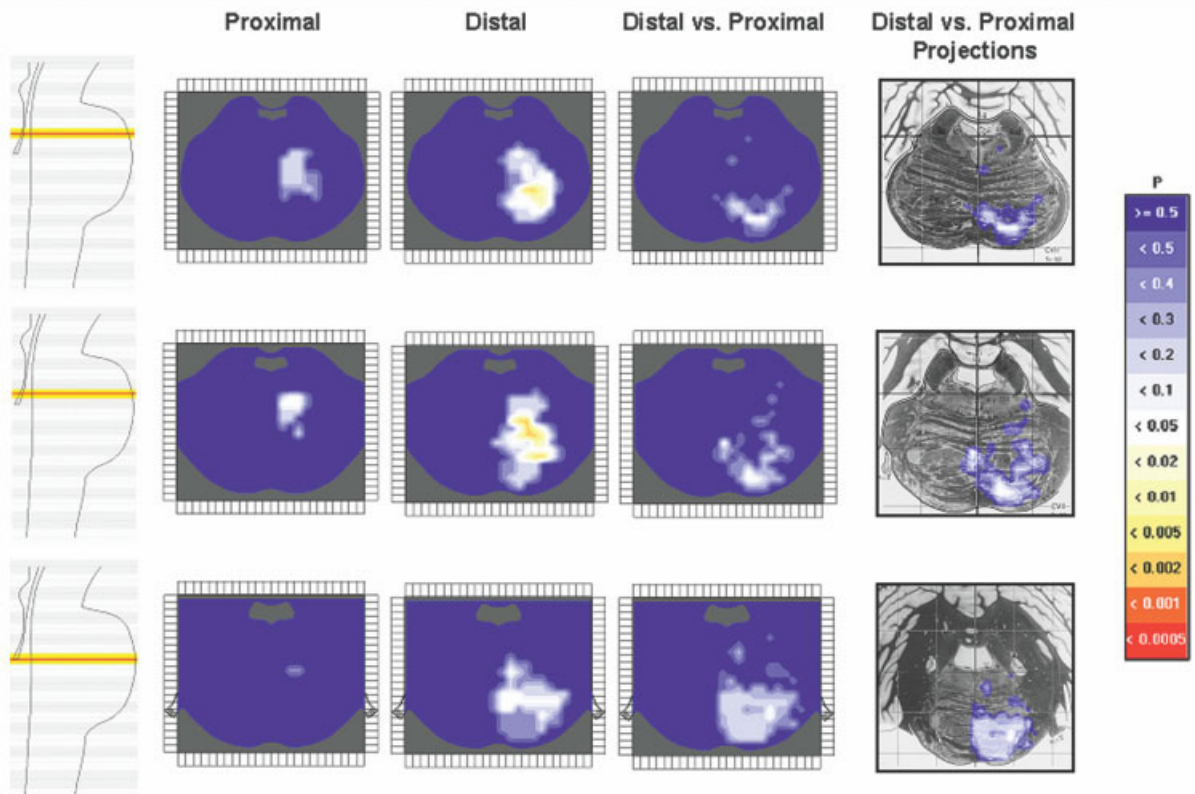


Fig 4. Color-coded probability maps on axial pontine sections of the three-dimensional brainstem model and projection on the corresponding slices of the anatomical atlas of Schaltenbrand and Wahren²¹ showing significantly affected voxels in patients with distal predominance of hemiparesis (χ^2 test), in patients with proximal predominance of hemiparesis (χ^2 test), and comparing patients with distal versus those with proximal predominance of hemiparesis (Mann-Whitney U test).

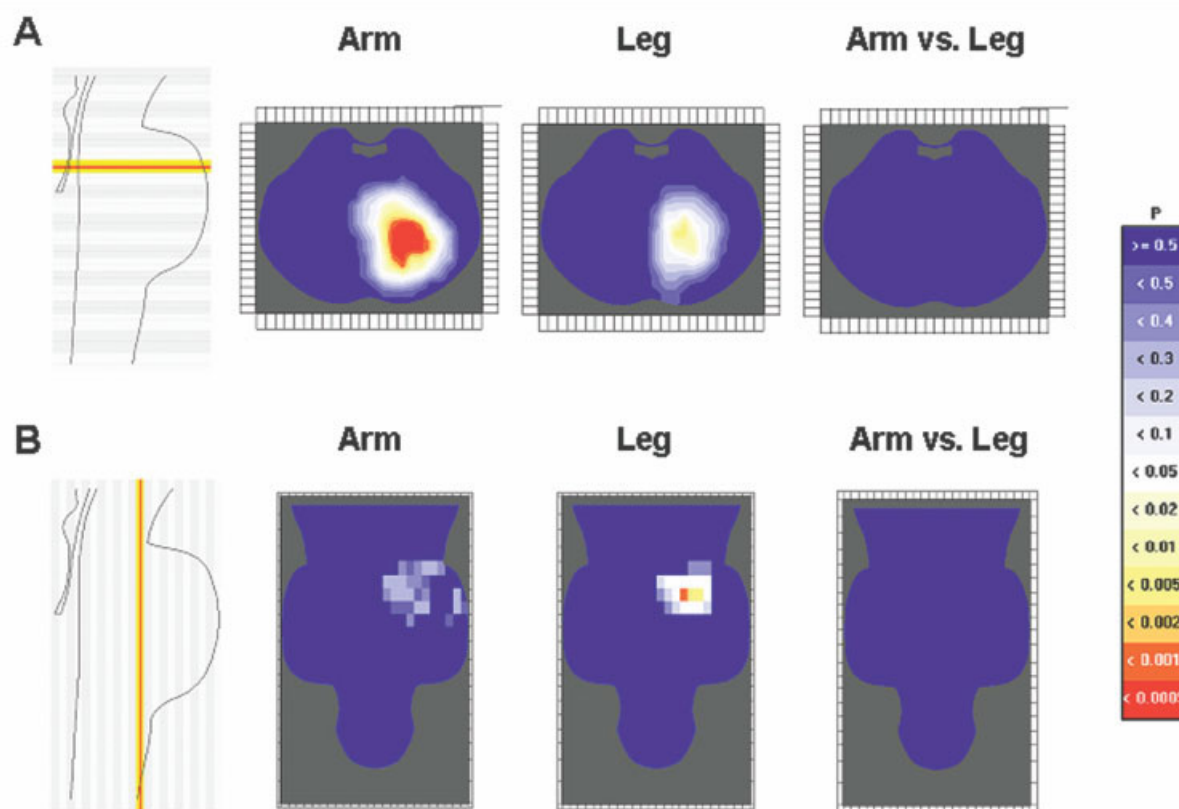


Fig 5. Color-coded probability maps on axial (A) and coronal (B) pontine sections of the three-dimensional brainstem model showing significantly affected voxels in patients with arm predominant hemiparesis (χ^2 test), in patients with leg predominant hemiparesis (χ^2 test), and comparing patients with leg versus those with arm predominant hemiparesis (Mann–Whitney U test).

pyramidal tract in the human brainstem.^{1,5,6} According to case studies mostly based on computed tomography and anatomical animal investigations, corticospinal fibers leave the cortex grouped in a somatotopic order.^{1,4,10} Systematic neighborhood relations of the descending tract appear to be maximum in the internal capsule, with fibers of the arm distributed anteromedially and fibers to the leg dorsolaterally. Based on primate lesion studies, however, this topographic arm/leg distribution appears to be progressively lost as the descending tract traverses the pons.^{10,12} In contrast, fibers appear to be randomly intermingled in the medullary pyramid and throughout the cervical tract of the spinal pathway. Nevertheless, in a recent MRI-based study on 16 retrospectively recruited patients with rostral lateral pontine infarction, the lesion responsible for crural monoparesis was presumed to be located in the dorsolateral pontine base.¹¹ In this study, however, no comparison with lesion location in patients with paresis predominantly affecting the arm was done.

Information on a possible somatotopic order of fibers supplying more proximally or distally located muscles in the human brainstem infarction is even more notional, with an assignment of lesions in more proximal paresis of the leg to lesions of or near the corticoreticular

tract.^{4,11} According to autoradiographic tracer and lesion studies, especially in the rhesus monkey, lesions of lateral brainstem areas in the lower pons and medulla oblongata lead to impairment of distal extremity and hand movements, whereas interruption of more medial brainstem systems results in an impairment of axial and proximal extremity movements.^{13–15}

In our fairly large cohort of prospectively recruited patients investigated by standardized high-resolution MRI, we applied a quantitative approach to study a possible somatotopic order of corticospinal fiber tracts. Hemiparesis was assessed not only clinically, but also with the recording of MEPs. We observed that motor hemiparesis in patients with brainstem infarction is almost exclusively caused by lesions affecting the pons. This is supposedly because of the ventral location of the pyramidal tract in the pons, where, according to anatomical correlation studies,⁸ ischemia is most frequent after occlusion of anteromedial pontine arteries (*Arteriae paramedianae* of Foix and Hillemand). Despite the high number of pontine infarctions, we could not find any significant difference in pontine lesion location between patients with a predominantly arm paresis and those with a predominantly leg paresis. There was an area significantly affected by lesions causing arm

predominant hemiparesis in the pons, but the lesions causing leg paresis appeared to be located above, within, and below it (especially in the coronal view), and the direct comparisons between the two groups did not yield any significance.

On the one hand, these results underline the need for statistically based analysis when doing functional anatomical correlations. Pure description of lesion location in a group of patients with a clinical deficit caused by infarction may reflect only the preferred territory due to the vascular supply. It does not allow decision if this area is actually important for the suspected function. On the other hand, this confirms the observations in primates where a topographic arm/leg distribution appears to be abruptly broken down as the descending corticospinal tract traverses the pons and fibers appear to be progressively intermingled downwards.^{10,12} In the upper pons near the pontomesencephalic junction, the expected topographic order of fibers supplying the arm anterolaterally and of fibers supplying the leg dorsolaterally may have not reached statistical significance because of the small number of patients with mesencephalic lesions.

In this study, lesion location was significantly more dorsal in patients with a predominantly proximal muscle weakness and was significantly more ventral in patients with a predominantly distal muscle weakness. Statistical significance for this differentiation was reached only in the pons, which is again most likely because of the predominance of pontine lesions in our cohort. Consistent with previous imaging correlation studies, a proximal predominance (especially for the lower limb) is seen in patients with a lesion extending dorsally to the corticoreticular tract in the pontine tegmentum.^{4,11} More ventral small lesions sparing the corticoreticular tract cause more severe weakness in distal muscles. That lesion location in patients with predominantly distal paresis was also slightly more lateral in the pons than that in patients with more proximal muscle weakness may contribute to the postulations after lesion and tracer studies in the rhesus monkey by Kuypers and colleagues.^{13–15} Here, descending pathways to the spinal cord were grouped according to their termination pattern in the spinal gray matter forming a medial and a lateral system in the lower brainstem. According to lesion studies, interruption of the lateral brainstem system produced impairment of distal extremity and hand movements, and interruption of the medial system resulted in an impairment of axial and proximal extremity movements. Kuypers and colleagues,^{13–15} however, refer especially to the lower brainstem, where we are unable to draw convincing topographic conclusions because of the small number of lesions in the lower pons and medulla oblongata in our population. Hence, at least a moderate degree of corticospinal tract somatotopy is still maintained in the pons.

Our method of statistically analyzing neuroimaging

data of patients with and without a given dysfunction is an innovative approach to in vivo correlation studies, because it minimizes the risk for highlighting vascular territories, rather than the structures specifically responsible for the clinical dysfunction, by comparing lesion topography in patients with and without the investigated clinical variable. However, it does not ignore completely the vascular supply to the brainstem. In earlier investigations, the method proved to identify functional areas that do not respect vascular territories such as the complete brainstem pathway of the early blink reflex component.^{16–18} Because the study is based on ischemic brainstem lesions only, it is apparently more difficult to make refined topodiagnostic assignments in brainstem areas that are rarely affected by ischemia as compared with the situation in the ventral pons or the dorsolateral medulla oblongata where brainstem infarction is more frequent.

Further studies collecting a larger number of patients with midbrain or medullary lesions may help to clarify the somatotopic organization of the corticospinal tract in the whole brainstem. However, because of the overrepresentation of pontine infarctions in our fairly large cohort of patients with brainstem infarction and motor hemiparesis, this is going to be a challenging task.

The study was supported by the DFG (Deutsche Forschungsgemeinschaft; Ho 293/10-1, J.J.M., S.F., P.S., H.C.H.).

References

1. Rondot P. Motor function. In: Vinken PJ, Bruyn GW, eds. Handbook of clinical neurology. Vol 1. Amsterdam: North-Holland, 1969:147–168.
2. Englander RN, Netsky MG, Adelman LS. Location of human pyramidal tract in the internal capsule: anatomic evidence. *Neurology* 1975;25:823–826.
3. Fisher CM, Ojemann RG. A clinico-pathologic study of carotid endarterectomy plaque. *Rev Neurol (Paris)* 1986;142:573–589.
4. Schneider R, Gautier JC. Leg weakness due to stroke. Site of lesions, weakness patterns and causes. *Brain* 1994;117:347–354.
5. Kubik CS, Adams RD. Occlusion of the basilar artery—a clinical and pathological study. *Brain* 1946;69:73–121.
6. Cravioto H, Rey-Bellet J, Prose PH, et al. Occlusion of the basilar artery. A clinical and pathological study of 14 autopsied cases. *Neurology* 1958;8:145–152.
7. Ferbert A, Brückmann H, Drummen R. Clinical features of proven basilar artery occlusion. *Stroke* 1990;21:1135–1142.
8. Bassetti C, Bogousslavsky J, Barth A, et al. Isolated infarcts of the pons. *Neurology* 1996;46:165–175.
9. Cavazos JE, Bulgara K, Caress J, et al. Pure motor hemiplegia including the face induced by an infarct of the medullary pyramid. *Clin Neurol Neurosurg* 1996;98:21–23.
10. Dawnay NA, Glees P. Somatotopic analysis of fibre and terminal distribution in the primate corticospinal pathway. *Brain Res* 1986;26:115–123.
11. Kataoka S, Miaki M, Saiki M, et al. Rostral lateral pontine infarction: neurological/topographical correlations. *Neurology* 2003;61:114–117.

12. Dawney NA, Glees P. Mapping the primate corticospinal pathway. *J Anat* 1981;133:124–126.
13. Kuypers HGJM, Fleming WR, Farinholt JW. Subcorticospinal projections in the rhesus monkey. *J Comp Neurol* 1962;118:107–137.
14. Lawrence DG, Kuypers HGJM. The functional organization of the motor system in the monkey. II. The effects of lesions of the descending brainstem pathways. *Brain* 1968;91:15–32.
15. Kuypers HGJM, Brinkmann J. Precentral projections to different parts of the spinal intermediate zone in the rhesus monkey. *Brain Res* 1970;24:29–48.
16. Marx JJ, Iannetti GD, Mika-Gruettner A, et al. Topodiagnostic investigations on the sympathoexcitatory brain stem pathway using a new method of three dimensional brain stem mapping. *J Neurol Neurosurg Psychiatry* 2004;75:250–255.
17. Cruccu G, Marx JJ, Iannetti GD, et al. Brainstem reflex circuits revisited. *Brain* 2005;128:386–394.
18. Thömke F, Marx JJ, Iannetti GD, et al. A topodiagnostic investigation on body lateropulsion in medullary infarcts. *Neurology* 2005;64:716–718.
19. Urban PP, Hopf HC, Zorowka PG, et al. Dysarthria and lacunar stroke: pathophysiological aspects. *Neurology* 1996;47:1135–1141.
20. Urban PP, Wicht S, Vucurevic G, et al. The course of corticofacial projections in the human brainstem. *Brain* 2000;124:1866–1876.
21. Schaltenbrand G, Wahren W. Atlas for stereotaxy of the human brain. Stuttgart: Thieme, 1977.
22. Capozza M, Iannetti GD, Mostarda M, et al. Three-dimensional mapping of brainstem functional lesions. *Med Biol Eng Comput* 2000;38:1–6.
23. Kretschmann HJ, Weinrich W. Neurofunctional systems—3D reconstructions with correlated neuroimaging. Stuttgart: Thieme, 1998.
24. Paxinos G, Huang XF. Atlas of the human brainstem. San Diego: Academic Press, 1995.
25. Matsumoto S, Okuda B, Imai T, et al. A sensory level on the trunk in lower lateral brainstem lesions. *Neurology* 1988;38:1515–1519.